SCIENTIFIC COMMITTEE
FIFTEENTH REGULAR SESSION

Pohnpei, Federated States of Micronesia
12-20 August 2019

Standardized catch per unit effort (CPUE) of skipjack tuna of the Japanese pole-and-line fisheries in the WCPO from 1972 to 2018

WCPFC-SC15-2019/SA-WP-14

Kinoshita, J., Aoki, Y., Ducharme-Barth, N. and Kiyofuji, H.

Standardized catch per unit effort (CPUE) of skipjack tuna of the Japanese pole-and-line fisheries in the WCPO from 1972 to 2018

WCPFC-SC15-2019/SA-WP-14

Kinoshita, J.[1], Aoki, Y.[2], Ducharme-Barth, N.[3] and Kiyofuji, H.[2]

[1]Research Center for Fisheries Resources, National Research Institute of Fisheries Science, Japan Fisheries Research and Education Agency, Yokohama, Kanagawa, Japan.

[2]National Research Institute of Far Seas Fisheries, Japan Fisheries Research and Education Agency, Shimizu-ku, Shizuoka-shi, Shizuoka 424-8633 Japan.

[3]Oceanic Fisheries Programme, The Pacific Community

Summary

Catch per unit effort (CPUE) of skipjack caught by Japanese pole-and-line fishing vessels (JPNPL) in two spatial structures (the same as used in the 2016 stock assessment (SA) and the alternative spatial structure for 2019 SA) was estimated from logbook data between 1972 and 2018. Three years of data from 2016 to 2018 were added since the 2016 SA, although 2018 data input are only about 75% completed so far. Two estimation methods were used: the GLM method (delta-GLM) and model configuration for estimating standardized CPUE used previously for the 2016 SA; and an extension of the 2016 SA model configuration in the form of a geostatistical delta-GLMM (geostats). Additionally, two versions of data screening procedures (SP) related to the model inputs were investigated; short cruises less than five days were removed (SP1) as occurred for the 2016 SA, or not removed (SP2). In the 2016 SA spatial structure, overall trends of standardized CPUEs calculated here were similar to the results of the 2016 SA in every region in spite of different SP inputs. As for the alternative spatial structure, standardized CPUEs obtained from SP1 were unable to be run because of data limitation; on the other hand, those derived from SP2 showed reasonable trends with inter-regional similarity among regions 2 (temperate area), 4 (northern subtropical area), 7 and 8 (tropical area). Comparison between the delta-GLM and geostats indices showed similar regional trends in both spatial structures.

Introduction

This document describes the standardization of catch per unit effort (CPUE) of skipjack tuna caught by Japanese pole-and-line fisheries (referred to as JPNPL) in the WCPO using logbook data from 1972 to 2018 with two spatial structures (**Fig.1**) and the same model configuration as used in the 2016 stock assessment (SA). Standardized JPNPL CPUE is important as an index that represents skipjack abundance and as an input data for a skipjack SA model for the WCPO. It was calculated in this document as delta-lognormal GLM (and GLMM) indices by multiplying

the set of indices obtained from the proportion of non-zero catch (by a binomial model) and the value of non-zero catch (by a lognormal model) (Lo et al., 1992, Langley et al., 2010; Kiyofuji et al., 2011; Kiyofuji and Okamoto, 2014; Kiyofuji, 2016). JPNPL fleets were divided into offshore pole-and-line (OS) and distant water pole-and-line (DW) according to vessel size, which affects their fishing strategy. OS operations consist of short cruises of less than two weeks during a fishing season from April through December, and their main fishing ground is distributed offshore of Tohoku, Japan (north of 30° N) (**Fig.2**). In contrast, DW fishing cruises may be longer than a month and fish throughout the year with a wide fishing ground in the WCPO (**Fig.3**).

Data and Methods

Fisheries Data

The JPNPL logbook data are available for the period from 1972 to 2018, although data input of 2018 has only been completed for about 75% of logbooks. The spatio-temporal resolution of the logbook data is 1 arc-degree at noon position (equal to 1×1° grid cells) and daily. The following information were employed for the CPUE calculation: date, skipjack catches in weight, number of poles, GRT, fishing device, and vessel identity. In this document, JPNPL was categorized by vessel size and their equipment. Vessel size between 20 and 199 GRT is defined as OS; vessel size equal to or greater than 200 GRT is defined as DW.

Historical transitions in the spatial patterns of OS and DW of JPNPL catch are shown in **Fig.2** and **Fig.3**, respectively. Recent fishing areas of reported catch diminished from that of the 1980s for both OS and DW fleets. In recent years the fishing areas of OS (**Fig.2**) have occurred almost exclusively within region 1 (the northmost region) in the 2016 SA spatial structure (**Fig.1(a)**). On the other hand, the DW fleet fished in region 1 and 2 (an equatorial region) (**Fig.3**). In the alternative spatial structure, which has been slightly modified from the one suggested by Kinoshita et al. (2018) based on discussions between SPC and NRIFSF, the reported catch areas of OS were categorized in region 1, 2 and 3 (**Fig.2**) and that of DW were categorized in region 2, 3, 4, 7, and 8 (**Fig.3**). **Fig.4(b)** shows time series of skipjack catch for OS and DW and the catch ratio of DW to the total catch of OS and DW. The decreasing trend of the catch starting in 1980s is shown in the time series.

Information on the fishing technology (i.e., fishing devices) used in JPNPL has been collected via interview, as described in Shono and Ogura (2000). The implementations of important technological innovations are available only in the DW fleets, these are (1) low temperature live bait tank (LTLBT), (2) the first and second generations of bird radar, (3) sonar, and (4) onboard NOAA meteorological satellite image receiver (NOAA receiver). The application of these

components is described in detail in Ogura and Shono (1999).

Vessel identification is effective, and is necessary information to remove bias of vessel effects, but there is no powerful identifier to trace back the current vessels to 1972 in the original JPNPL logbook data. Thus, we assigned vessel ID using the fishing license number, which is unique to a vessel and is changed every five years (1987, 1992, 1997 and so on). A reference table has been created and updated which details the historical succession of the license number of every vessel (Langley et al., 2010; Kiyofuji et al., 2011 and 2014). The assignment rules for vessel ID are shown below.

1. Discrete vessel ID is assigned for each vessel by combining a ship's register prefecture (29 prefectures hold skipjack fisheries in Japan) and a ship name. Therefore, the same vessel ID is sustained as long as the combination is the same even if the condition of the ship changes (purchased, transferred, or new ship constructed) or the fishery license type switches (e.g. from offshore to distant water), which applies to the most cases.
2. For the vessels that have the same register prefecture, the same ship name, and the same fishery license type in the same year but have different GRT, discrete vessel IDs are assigned by adding GRT information, which occurs rarely.

It should be noted that vessel ID assigned by the rules above should not be assumed as a ship-specific ID (such as IMO identification number) because vessel ID was not always connected to a particular ship but rather connected to a fishery body (e.g., a fishing company, a family or a person who owns the vessel) so that we consider the vessel ID as a fishery unit.

Data screening

The integrated data based on the original logbooks were adopted in the model following the procedures of filtering according to regions as below. The procedures followed that of the 2016 SA (Kiyofuji 2016).

(Binomial and lognormal model parts)

Filter 1. Remove data NOT included in any defined region

Filter 2. Remove data of a cruise where the proportion of skipjack catch during a cruise was less than 75% of the combined catch of skipjack and albacore

Filter 3. Remove data of a cruise that lasted less than five days

Filter 4. Remove data of a vessel that had operated for less than 5 years and less than 10 days per year

Filter 5. Remove data of a vessel that had no vessel IDs assigned in and after 1987, when

fishing license numbers changed substantially

Filter 6. (For DW only) Remove data that have unknown device information

(For lognormal model part)

Filter 7. Remove zero skipjack catch records

Filter 8. Remove extremely high skipjack catch records of over 200 tons per day

In the 2016 skipjack SA, sensitivity runs for the alternative spatial structure were planned and thus CPUEs for these models should also be standardized. CPUE indices were standardized for both the regions of the 2016 SA and the alternative spatial structure, as shown in **Fig.1**. However, data were substantially removed in the process of Filter 3, especially for the OS fleet (**Fig.5a**, **b**). Thus, input data for models were created for two cases; Filter 3 employed (screening procedure 1, hereafter called SP1) and Filter 3 not employed (screening procedure 2, hereafter called SP2). Details of data type of the model input are shown in **Table 1.**

Fig.6 and **Fig.7** represent active duration of every vessel ID in each region in the 2016 SA and the alternative spatial structure. Discontinuance of fishing operations of fishery units (vessel ID) started in 1990's and approximately 50–60% of units had closed their business. Furthermore, in the 1980s many JPNPL were converted to the purse seine fishery as policy had been changed due to deterioration of PL management of each fishery unit. Hence, the data that were influenced by these changes in the skipjack fishery might have some impacts on the standardization process and results.

Model configuration: delta-GLM

Generalized linear models (GLMs) fitted using R (R core team, 2018) were used to standardize CPUE. The followings are basic equations applied for JPNPL DW and OS, respectively.

$$CPUE(OS) = YearQtr + VesselID + LatLong + NumPoles + \mu$$
$$CPUE(DW) = YearQtr + VesselID + LatLong + NumPoles + Device + \mu$$

Definitions of the predictor variables are shown in **Table 2** and **Table 3**. Device refers to either bait tank (BT), bird radar (BR), sonar (SN), and or NOAA receiver (NOA). GLMs were carried out separately for each region and for each model part (binomial and lognormal).

The proportion of non-zero skipjack catch for a fishing day was used to obtain the dependent variables that were modeled using a binomial error structure to estimate probability of non-zero skipjack catch. The value of non-zero skipjack catch for a fishing day was calculated after

removing zero catch records. The dependent variable was modeled assuming a lognormal error structure. For the binomial model, the year/quarter indices for probability of capture (p) were derived by the inverse logit transformation of the individual year/quarter factorial coefficients, with the average predicted value of p in the first 5 years constrained to equal the observed average p in the same period. For the lognormal model, the year/quarter CPUE indices were derived by the exponentiation of the individual year/quarter factorial coefficients. Delta-lognormal indices were derived by multiplying the binomial p values and the non-zero lognormal indices (Lo et al., 1992). These indices were calculated individually for OS and DS since they have different fishing strategies.

A list of the final model configurations is shown in **Table 4** used for every region with the 2016 SA definition and the alternative regional definition. As for updated data, two results were derived from different input data created by SP1 or SP2.

Model configuration: geostatistical delta-GLMM

Based on the findings of Ducharme-Barth et al. (2019), a geostatistical extension of the delta-GLM was implemented as a delta-GLMM using version 5.4.0 of the VAST package (Thorson et al., 2015; Thorson 2019) in R (R core team, 2018). Using this framework allowed for a joint analysis of the DW and OS data, and allowed for the simultaneous estimation of all the regional abundance indices using a single model. The basic equations applied are as follows for each model part (binomial and lognormal):

$$p_i \sim YearQtr + VesselID + \omega_1(x_i) + \phi_1(x_i, t_i) + Class + s(NumPoles) + s(grt) + \xi_1(x_i, t_i)$$

$$c_i \sim YearQtr + VesselID + \omega_2(x_i) + \phi_2(x_i, t_i) + Class + s(NumPoles) + s(grt) + \xi_2(x_i, t_i)$$

where $YearQtr$ is a fixed effect, $VesselID$ is a normally distributed random effect, $\omega(x_i)$ is the spatial random effect at knot x associated with logsheet record i, $\phi(x_i, t_i)$ is the spatiotemporal random effect at $YearQtr\ t$ and knot x, *Class* is a fixed effect denoting a vessel as either OS or DW, $s(NumPoles)$ is a polynomial spline of degree 5 for the number of poles fished, $s(grt)$ is a polynomial spline of degree 5 for the vessel size, and $\xi(x_i, t_i)$ is the linear effect of sea surface temperature (SST; Smith and Reynolds 1981) at $YearQtr\ t$ and knot x. Both ω and ϕ are described by multivariate normal spatial random fields $MVN(0, R)$ where R is a Matern correlation function. In the case of ϕ, temporal independence across *YearQtr* is assumed. Two-hundred-eighty spatial knots were used to define the spatial structure of the model, and these were distributed in proportion to the spatial density of the observations (**Fig. 8**). Please consult the *Technical Annex* of Ducharme-Barth et al. (2019) for a more thorough discussion of both the model structure and description of the process allocating observations to spatial knots.

One of the benefits of the geostats framework is that it can use the estimated spatial correlation structure of the data, along with any estimated relationships with environmental covariates, to interpolate abundance into un-sampled areas. However, for a tropical species like skipjack tuna, it is particularly important that biomass is not interpolated into areas that are biologically unfeasible (i.e. too cold). Previous geostats analyses, such as the one for 2018 albacore, made modifications to the geostats model to only use biomass from grid cells that met a biologically realistic minimum temperature threshold for the creation of the abundance index (Tremblay-Boyer et al. 2018). The same approach was taken in this analysis using the 18°C minimum thermal threshold found for skipjack tuna by Kiyofuji et al. (2019).

In addition to the differences in model equations, there are a few other key differences in the implementation of the delta-GLM and geostats models. In order to have more complete spatial-temporal coverage within the assessment model time period and region, DW and OS trips were combined in a joint analysis. In order to account for potential differences in catchability between the two vessel classes, the fixed effect of *Class* was added along with the polynomial spline of vessel size. Furthermore, preliminary analyses of the nominal CPUE in spatio-temporal strata that were fished by both DW and OS vessels showed similarities in the magnitude and trend of mean catch rates. Given the joint modeling approach of the DW and OS trips and the fact that device information was unavailable for OS vessels, device covariates (bait tank, bird radar, sonar and NOAA receiver) were not included in the geostats model. This was assumed to not present much of an issue as preliminary models fit just to the DW trips (where device information was available) showed that including device information had a negligible impact on the estimated index. Lastly, a slight modification of the SP2 screening procedure, where filter 2 was not applied, was used for the geostats analysis. The original rationale for applying this filter (Langley et al. 2010) was to exclude trips from the analysis that were targeting albacore in a different spatial area from where they were catching skipjack. Given that the geostatistical model allows for explicit spatial modeling of the observations, and that there is no fundamental difference in gear configuration between albacore and skipjack targeting; we felt that including observations of low skipjack catch provided value information on the distribution of skipjack abundance in the model.

Results and Discussion

Updated CPUE obtained from the 2016 SA Spatial Structure using the Delta-GLM model

Updated results of the probability of non-zero skipjack catch and indices of non-zero catch and abundance (i.e., the delta-lognormal index) are shown in **Fig.9** to **Fig.11**. Previous data (shown

as black lines) were presented as red lines in Figure 5 to 7 of Kiyofuji (2016). It should be noted that the trends of Figure 5 to 7 in Kiyofuji (2016) were calculated in the 2014 SA spatial structure. The spatial structure between 2014 and 2016 SAs were similar so that these were comparable with our results. Overall trends of these three indices in each region were consistent with the results of 2016 SA.

The binomial model indicated that the probabilities of non-zero catch were mostly between 0.8 and 1.0 for both fleets during the analysis period (**Fig.9**). OS fleets (only fishing in region 1) showed almost flat profiles while DW fleets (in region 1 to 3) showed a gradual decrease in all available regions from 1972 to the present day. In addition, the probability of non-zero catch of SP1 (shown as red lines in **Fig.9**) in the OS fleets was slightly low overall compared with those of previous analyses (black line) and SP2 (blue line).

The lognormal model indicated that the non-zero catch indices had no particular change in trend compared with the previous model. However, it was observed that a relatively low positive catch index in SP2 of OS fleet in region 1 until 1985 and a spike in updated indices of SP1 and SP2 of the DW fleets in region 3 in 2000 (**Fig.10**).

The abundance indices calculated by multiplying both the binomial and lognormal indices showed a similar trend with that of the non-zero catch, which had low abundance indices in both OS and DW fleets from 1972 to 1990 while they were higher from 1990 to 2005. After 2005, they tended to show a declining trend up to the present day (**Fig.11**).

The Alternative Spatial Structure in the 2019 SA using the Delta-GLM model

The results obtained from the alternative area definition, which were the probability of non-zero skipjack catch and indices of non-zero catch and abundance are shown in **Fig.12–Fig.14**. In contrast to the results of the 2016 SA spatial structure, some parts of the calculated results showed a clear difference coming from the input data difference (SP1 or SP2), which was obvious in the results of region 1 and 2 of OS fleets and region 3 of DW fleets. In the calculations of three indices, multiple years of unsuccessful estimation were observed when using the input data of SP1, thus hereafter we mainly focus on the trends obtained from the SP2 input data.

The binomial model in the alternative area definition indicated that the probabilities of non-zero catch were mostly between 0.6 and 1.0 for both fleets except for region 1 and 2 of the OS fleet and region 3 of DW fleet with the SP1 input data (**Fig.12**). In the case of SP2 (shown as the red line in **Fig.12**), the probability of non-zero catch of the OS fleet in region 1 and 2 gradually

increased from 0.7 to about 0.9 until 2000, and after that it gradually decreased till it reached 0.7 again. On the other hand, in region 3 of the OS fleet the trend was maintained high above 0.9 overall with gradual increase starting from 1980s (**Fig.12**). That of region 2 of the DW fleet indicated a sharp fall from 0.8 to 0.4 in the period between 1972 and 1981. After the fall, a rapid increase was observed that continued until 1985 and it stayed around 0.7 until 2000. A decreasing trend was again observed after 2000, and it has been around 0.5 in recent years. In region 3 of DW fleet, it had been around 0.9 from 1972 to 1983, and after that it was maintained around 0.8 with year-to-year fluctuations. In region 4, the non-zero catch probability of DW fleets showed an almost flat profile ranging between 0.8 to 0.9 from 1972 to 2007. It fluctuated around 0.7 until 2013, and slightly increased and it was around 0.8 after 2014. DW fleets in region 7 and 8 showed similar trends which are represented by the gradual decrease from about 1.0 to 0.9 starting from 1972 to date. (**Fig.12**).

The lognormal model in the alternative area definition indicated that the positive catch indices were clearly different between SP1 and SP2 in the OS fleet, on the other hand, they are similar in DW fleets (**Fig.13**). SP2 results (shown in red line in **Fig.13**) in region 1 and 2 of the OS fleet showed an increasing trend from 1972 to 2000 and the trend turned to be downward gradually. On the other hand, region 3 showed gradual increase from 1972 to the present time (**Fig.13**). The trend of region 2 of DW fleets were similar to that of the OS fleets. The flat trend was observed in region 3 of DW fleets though it fluctuated year-to-year (**Fig.13**). The differences between maximum and minimum values in region 4, 7 and 8 were smaller than that of region 2, though the trends were similar (i.e., a gradual increase until 2000 and following decreases afterwards).

The delta-lognormal model indicated that SP1 and SP2 derived different results in the cases of region 1 and 2 of OS fleets and region 3 of DW fleets (**Fig.14**). According to the SP2 results (shown in red line), region 1 of OS fleets showed gradual increase starting from the early 1970's which continued until around 2000, followed by a continuous decreasing trend. Region 2 of OS fleets had an increase in its index until the middle of 1990s, followed by a gradual decrease until recent years (**Fig.14**). Region 3 of OS fleets showed a gradual increase starting from 1972 to date. In region 2 of DW fleets in recent years showed a decreasing trend after the decrease around the early 1980s and the increase afterwards continued until around 2000. Region 3 of DW fleets showed a flat profile until the middle of 1990s with fluctuations between years. Afterwards, the index decreased until 2000. With a slight upward trend in the middle of 2000s, the index remained low after the 2000s (**Fig.14**). For region 4, the index increased until the middle of the 1990s and was almost flat until the late of 2000s. After that, the index remained low until the

early 2010s and showed a slight increasing trend to date (**Fig.14**). The results of region 7 and 8 of DW fleets had similar trends, and their high values in 1990s were also seen in region 2 and 4 (i.e., a gradual increase that continued until 2000 and with decreases following afterwards).

Geostatistical delta-GLMM and comparison to delta-GLM

Several clear patterns emerged from examining the results of the geostatistical model. In both the binomial and lognormal components of the model, vessel effect showed clear positive temporal trends (**Fig. 15**). Though the JPNPL fleet has diminished in size, these results appear to show an increase in per-vessel efficiency in both locating and catching skipjack, which might be expected in a fleet that is reducing in size, i.e. the less efficient vessels drop out first due to poor economic performance. This illustrates the importance of accounting for the vessel effect. Failing to do so could lead to hyperstability in the abundance index. Additionally, exploration of the spatial probability of encounter and predicted CPUE (**Fig. 16 & Fig.17**) shows the relationship between the Kuroshio extension current (~30N) and skipjack CPUE in the northern region. In the northern region, probability of encounter and CPUE of skipjack appear to be highest immediately to the north of the extension current. It is possible that vertical compression of skipjack due to a shallow thermocline has increased the catchability for skipjack in this region. Future research is needed to appropriately identify and account for this effect in the CPUE standardization.

Despite the differences in model structure, data modeled, and data filtration; the geostatistical indices are remarkably similar to the delta-GLM indices for both the 2016 SA areas (**Fig.18**) and the 2019 alternative spatial structure (**Fig. 19**). However, there were two instances (2016 SA region 1 and 2019 proposed region 3) where the trends appear to be different between the two model structures. For the delta-GLM, only OS trip data were used to calculate the indices in these two regions. Given that these regions showed differing trends between the OS and DW data from the delta-GLM analysis (**Fig. 11 & Fig. 14**), it is likely that the difference in trend between the delta-GLM and geostats indices for these regions is due to the joint modeling of the OS and DW data in the geostats approach.

The following is a summary of this document.

- Skipjack abundance indices obtained from the JPNPL fisheries in the WCPO were updated until 2018 using the same area definition (spatial structure) as the 2016 SA but data screening procedures were conducted according to two different patterns (SP1: same as 2016 SA, SP2: newly suggested).
- CPUEs for the alternative spatial structure were also estimated with SP1 and SP2 procedures

separately.

- No large changes were identified on the updated CPUE compared to the 2016 SA indices (which were conducted based on the 2014 SA area definition, strictly speaking).
- Different CPUE trends were identified between SP1 and SP2 in the alternative spatial structure. SP2 indices would be reasonable to explain the skipjack stock trend because some SP1 indices dropped off in some years.
- For the alternative spatial structure, the abundance index trends were similar among regions 2 (temperate area), 4 (northern subtropical area), 7 and 8 (tropical area).
- Indices did not differ greatly between the two modelling approaches: delta-GLM and geostatistical delta-GLMM.

Reference

Ducharme-Barth, N., Vincent, M., Pilling, G., and Hampton, J. (2019) Simulation analysis of pole and line CPUE standardization approaches for skipjack tuna in the WCPO. WCPFC-SC15-2019/SA-WP-04.

Kinoshita, J., Aoki, Y., Ijima, H., and Kiyofuji, H. (2018) Improvements in skipjack (*Katsuwonus pelamis*) abundance index based on the fish size data from Japanese pole-and-line logbook (1972–2017). WCPFC-SC14-2018/ SA-WP-04.

Kiyofuji, H., Uosaki, K. and Hoyle, S. (2011) Up-to-date CPUE for skipjack caught by Japanese distant and offshore pole and line fishery in the western and central Pacific Ocean. WCPFC-SC7-2011/SA-IP-13.

Kiyofuji, H. and Okamoto, H. (2014) An update of the standardized abundance index of skipjack by the Japanese pole-and-line fisheries in the WCPO. WCPFC-SC10-2014/SA-IP-16.

Kiyofuji, H. (2016) Skipjack Catch per unit effort (CPUE) in the WCPO from the Japanese pole-and-line fisheries. WCPFC-SC12-2016/ SA-WP-05.

Kiyofuji, H., Aoki, Y., Kinoshita, J., Okamoto, S., Masujima, M., Matsumoto, T., Fujioka, K., Ogata, R., Nakao, T., Sugimoto, N., and Kitagawa, T. (2019). Northward migration dynamics of skipjack tuna (Katsuwonus pelamis) associated with the lower thermal limit in the western Pacific Ocean. Progress in Oceanography 175, 55–67. https://doi.org/10.1016/j.pocean.2019.03.006

Langley, A., Uosaki, K., Hoyle, S., Shono, H., and Ogura, M. (2010) A standardized CPUE analysis of the Japanese distant-water skipjack pole-and-line fishery in the western and central Pacific Ocean (WCPO), 1972-2009. WCPFC-SC6-2010/SA-WP-08.

Lo, N. C. H., L. D. Jacobson, J. L. Squire, (1992) Indices of Relative Abundance from Fish Spotter

Data based on Delta-Lognormal Models. Canadian Journal of Fisheries and Aquatic Sciences, 49(12), 2515-2526.

Ogura, M. and Shono, H. (1999) Factors affecting the fishing effort of the Japanese distant water pole and line vessel and the standardization of that skipjack CPUE. Part A; Description of the fishery and the data. Standing Committee on Tuna and Billfish, SCTB12 SKJ-4, 1-12.

Shono and Ogura (2000) The standardized skipjack CPUE, including the effect of searching device, of the Japanese distant water pole and line fishery in the western central Pacific Ocean. Collective Volume for Science Papers, ICCAT, 51: 312-328.

Smith, T. and Reynolds, R. (1981). NOAA Smith and Reynolds Extended Reconstructed Sea Surface Temperature (ERSST) Level 4 Monthly Version 5 Dataset in netCDF. https://podaac.jpl.nasa.gov/dataset/REYNOLDS_NCDC_L4_MONTHLY_V5

Thorson, J. T., Shelton, A. O.,Ward, E. J., and Skaug, H. J. (2015). Geostatistical delta-generalized linear mixed models improve precision for estimated abundance indices for West Coast groundfishes. Ices Journal of Marine Science, 72(5):1297-1310.

Thorson, J. T. (2019). Guidance for decisions using the Vector Autoregressive Spatio-Temporal (VAST) package in stock, ecosystem, habitat and climate assessments. Fisheries Research, 210:143-161.

Tremblay-Boyer, L, S McKechnie, and G Pilling. (2018). Background Analysis for the 2018 Stock Assessment of South Pacific Albacore Tuna. WCPFC-SC14-2018/ SA-IP-07.

Table 1. Included data for model input for each model part and screening procedure

Model part	SP1	SP2
Binomial	Remain + f7 + f8	Remain + f3 + f7 + f8
Lognormal	Remain	Remain + f3

Remain presents the remaining data after all the filtering steps applied (details are mentioned in the text). The abbreviations of f3, f7, and f8 indicate data that would be filtered by Filter 3, Filter 7, and Filter 8, respectively.

Table 2. Definition of the predictor variables included in the model for JPNPL OS fleets (GRT < 200)

Variables	Data type	Description
YearQtr	Categorical	Unique year and quarter
LatLong	Categorical	Aggregated to 5°×5° grid cell (latitude x longitude)
VesselID	Categorical	Vessel ID (assigned by the authors)
NumPoles	Continuous	Number of poles (used by cubic spline interpolation in models)

Table 3. Definition of the predictor variables included in the model for JPNPL DW fleets (GRT >= 200)

Variables	Data type	Description
YearQtr	Categorical	Unique year and quarter
LatLong	Categorical	Aggregated to 5°×5° grid cell (latitude x longitude)
VesselID	Categorical	Vessel ID (assigned by the authors)
NumPoles	Continuous	Number of poles (used by cubic spline interpolation in models)
Bait Tank (BT)	Categorical	1. Vessel does not have LTLBT*
		2. Vessel has LTLBT*
Bird Radar (BR)	Categorical	1. Vessel does not have any bird radar of any generation
		2. Vessel has a 1st or 2nd generation bird radar
Sonar (SN)	Categorical	1. Vessel does not have sonar
		2. Vessel has sonar
NOAA receiver (NOA)	Categorical	1. Vessel does not have NOAA receiver
		2. Vessel has NOAA receiver

* LTLBT: low temperature live bait tank

Table 4. Summary of the final model configurations of JPNPL CPUE estimations used in the 2016 SA and 2019.

		2016 SA area				Alternative area	
Region No.	Model part	2016 SA data (All)		2019 SA data SP1/SP2		2019 SA data SP1/SP2	
		OS	DW	OS	DW	OS	DW
1	Binomial	(2)	-	(2)/(2)	(12)/(11)	(1)/(2)	-
	Lognormal	(2)	-	(2)/(2)	(6)/(6)	(2)/(2)	-
2	Binomial	-	(5)	-	(8)/(8)	(2)/(2)	(8)/(8)
	Lognormal	-	(10)	-	(12)/(6)	(2)/(2)	(8)/(8)
3	Binomial	-	(4)	-	(1)/(2)	(1)/(2)	(9)/(1)
	Lognormal	-	(7)	-	(6)/(6)	(2)/(2)	(3)/(3)
4	Binomial	-	-	(1)/(1)	-	-	(2)/(2)
	Lognormal	-	-	(2)/(2)	-	-	(14)/(2)
5	Binomial	-	-	-	-	-	-
	Lognormal	-	-	-	-	-	-
6	Binomial					-	-
	Lognormal					-	-
7	Binomial					-	(8)/(8)
	Lognormal					-	(13)/(13)
8	Binomial					-	(1)/(1)
	Lognormal					-	(6)/(13)

(1) YearQtr + LatLong + VesselID
(2) YearQtr + LatLong + VesselID + poly(NumPoles, 3)
(3) YearQtr + LatLong + VesselID + BT
(4) YearQtr + LatLong + VesselID + BR
(5) YearQtr + LatLong + VesselID + SN
(6) YearQtr + LatLong + VesselID + poly(NumPoles, 3) + BT
(7) YearQtr + LatLong + VesselID + poly(NumPoles, 3) + BR
(8) YearQtr + LatLong + VesselID + poly(NumPoles, 3) + SN
(9) YearQtr + LatLong + VesselID + poly(NumPoles, 3) + NOA
(10) YearQtr + LatLong + VesselID + poly(NumPoles, 3) + BT + BR
(11) YearQtr + LatLong + VesselID + poly(NumPoles, 3) + BT + SN
(12) YearQtr + LatLong + VesselID + poly(NumPoles, 3) + BT + NOA
(13) YearQtr + LatLong + VesselID + poly(NumPoles, 3) + BT + BR + NOA
(14) YearQtr + LatLong + VesselID + poly(NumPoles, 3) + BT + BR + SN

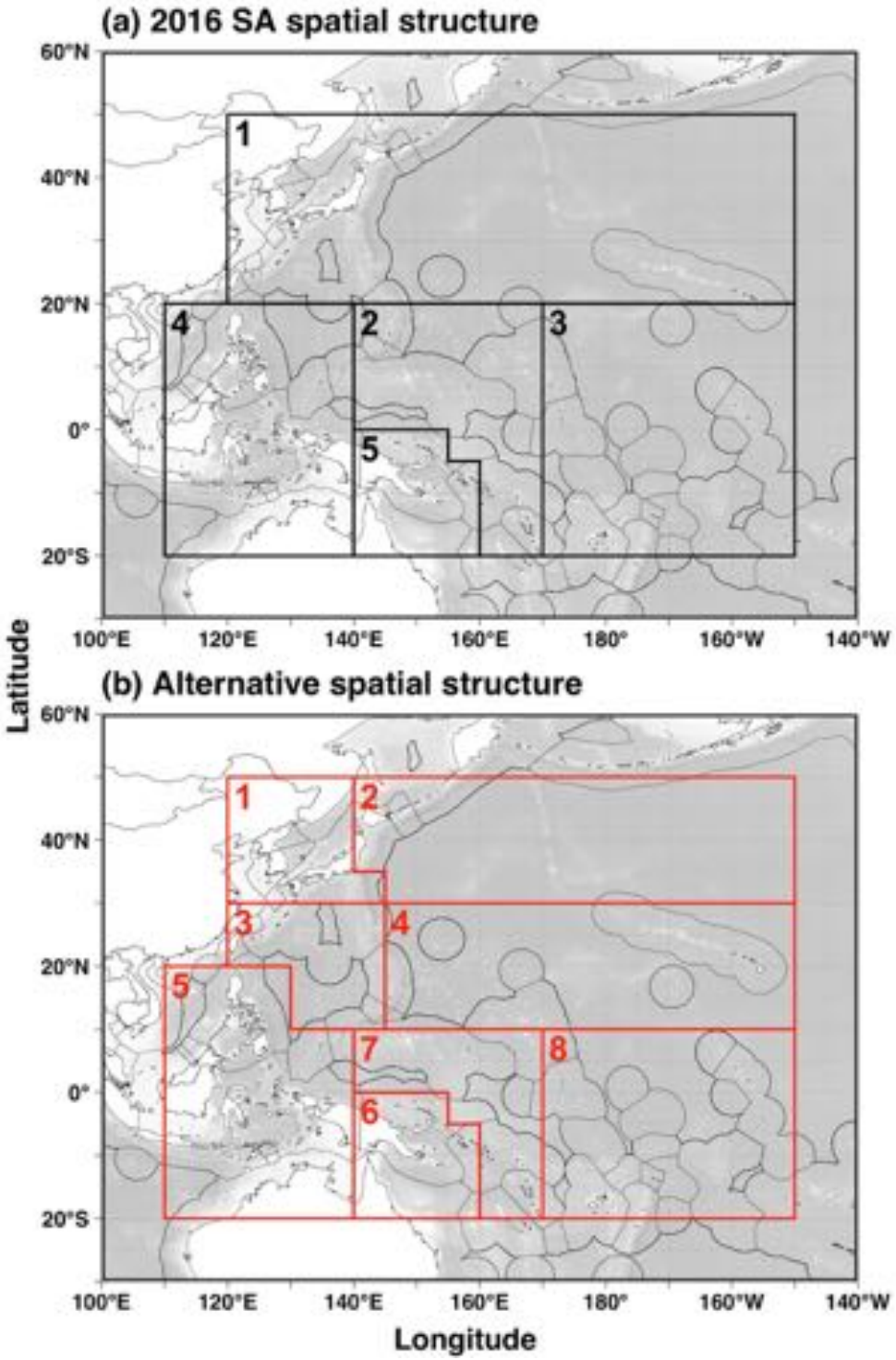

Figure 1. Spatial structures of the (a) 2016 SA and (b) the alternative area structure.

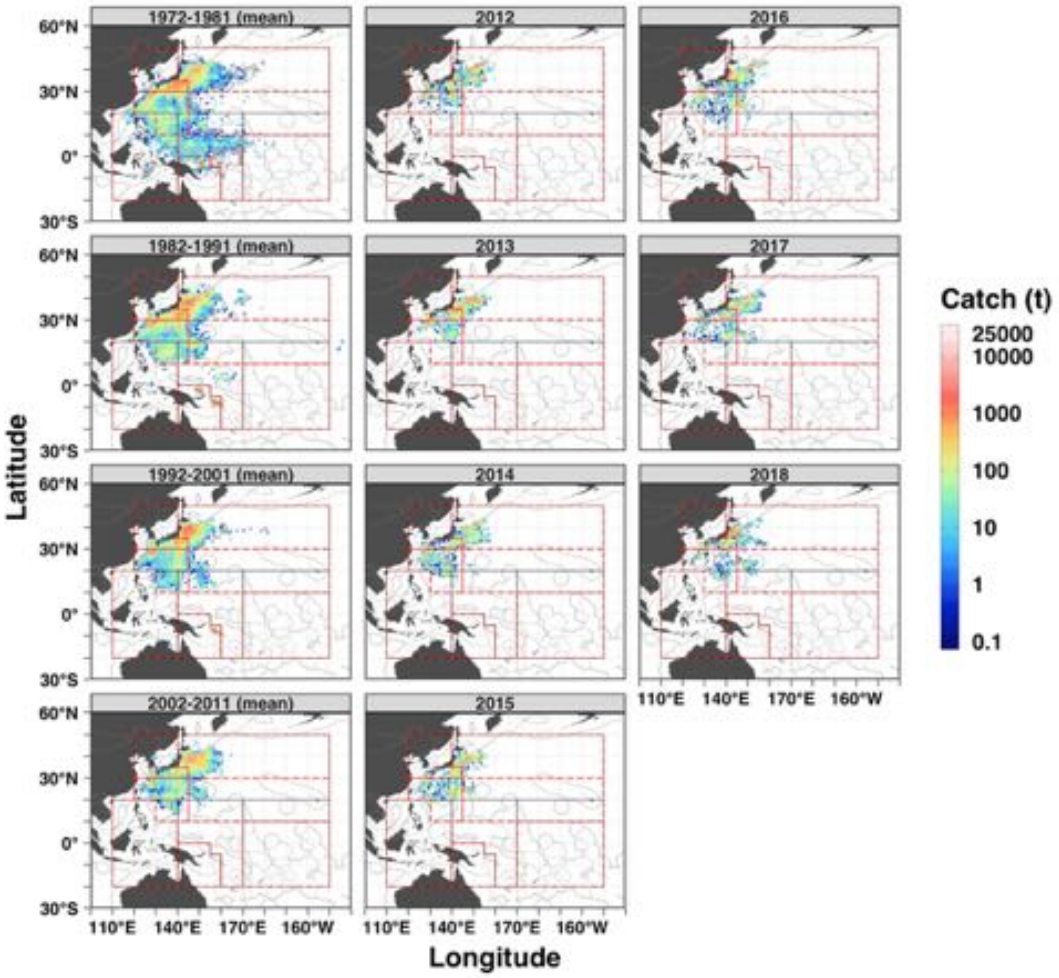

Figure 2. Spatial distribution of skipjack catches by Japanese offshore pole-and-line fisheries (JPNPL OS). Mean was calculated as decadal mean.

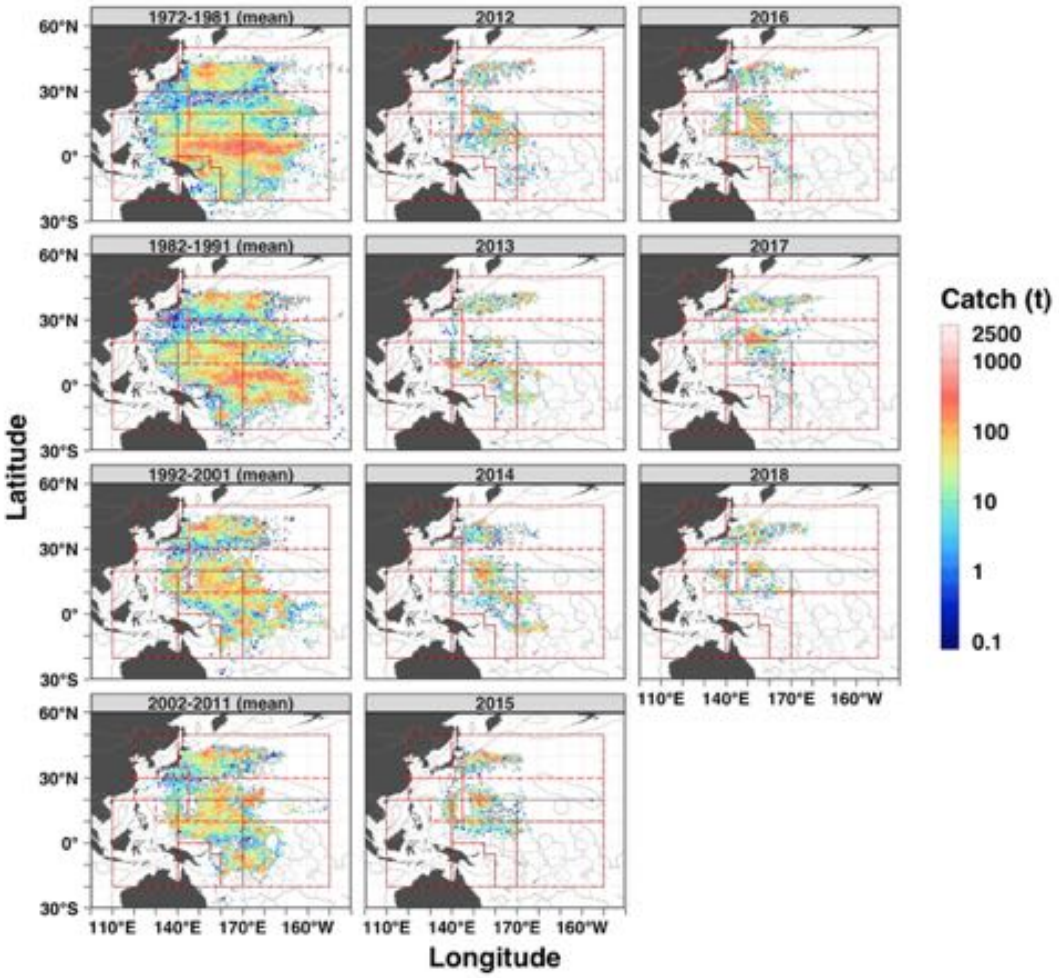

Figure 3. Spatial distribution of skipjack catches by Japanese distant water pole-and-line fisheries (JPNPL DW). Mean was calculated as decadal mean.

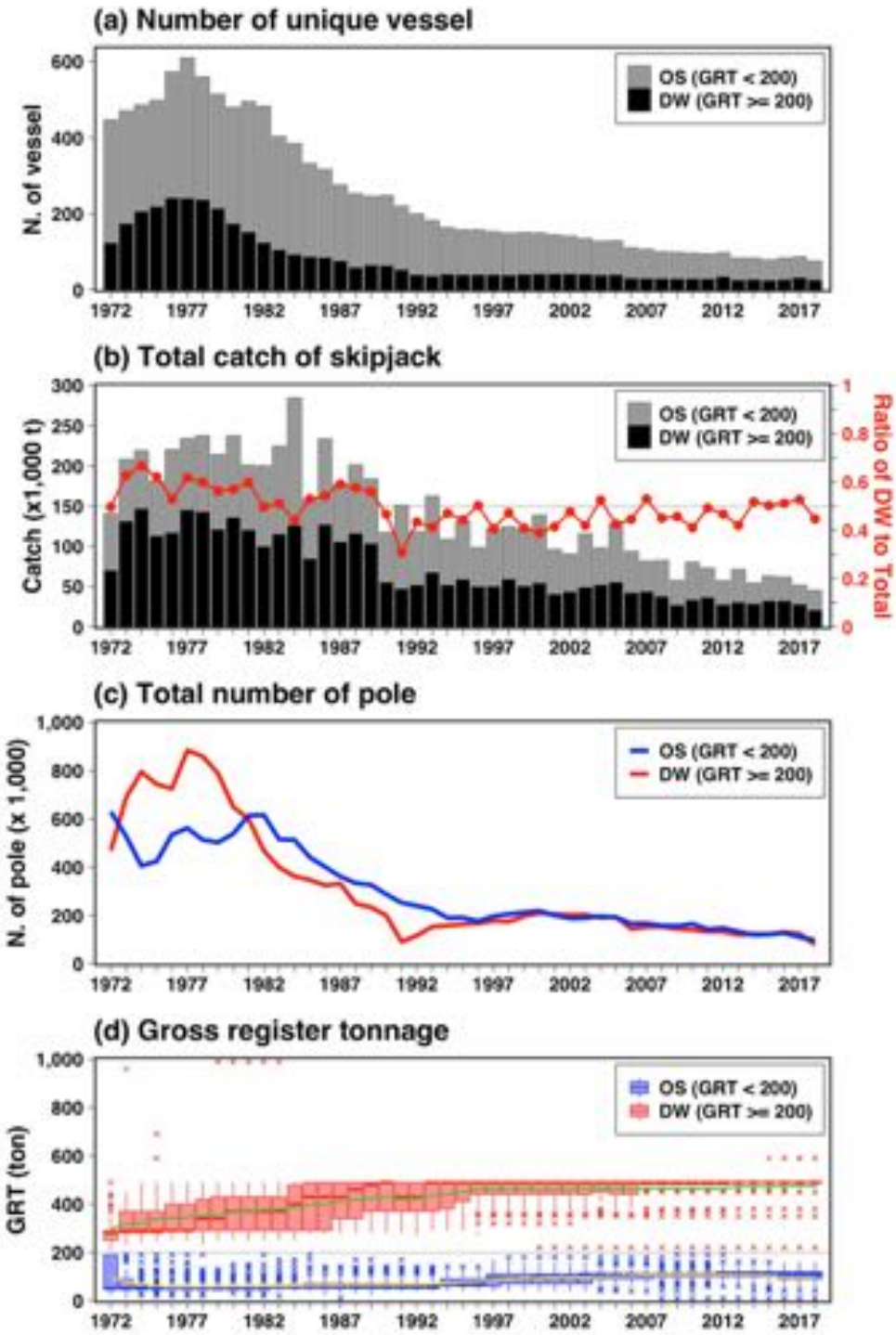

Figure 4. Time series data representing the history of two fleets (JPNPL DW and JPNPL OS); (a) number of unique vessels, (b) skipjack catch by DW and OS and the ratio of DW catch to the total (c) total number of poles, and (d) transition of the gross register tonnage (GRT) (green line: average of DW GRT; yellow line: average of OS GRT)

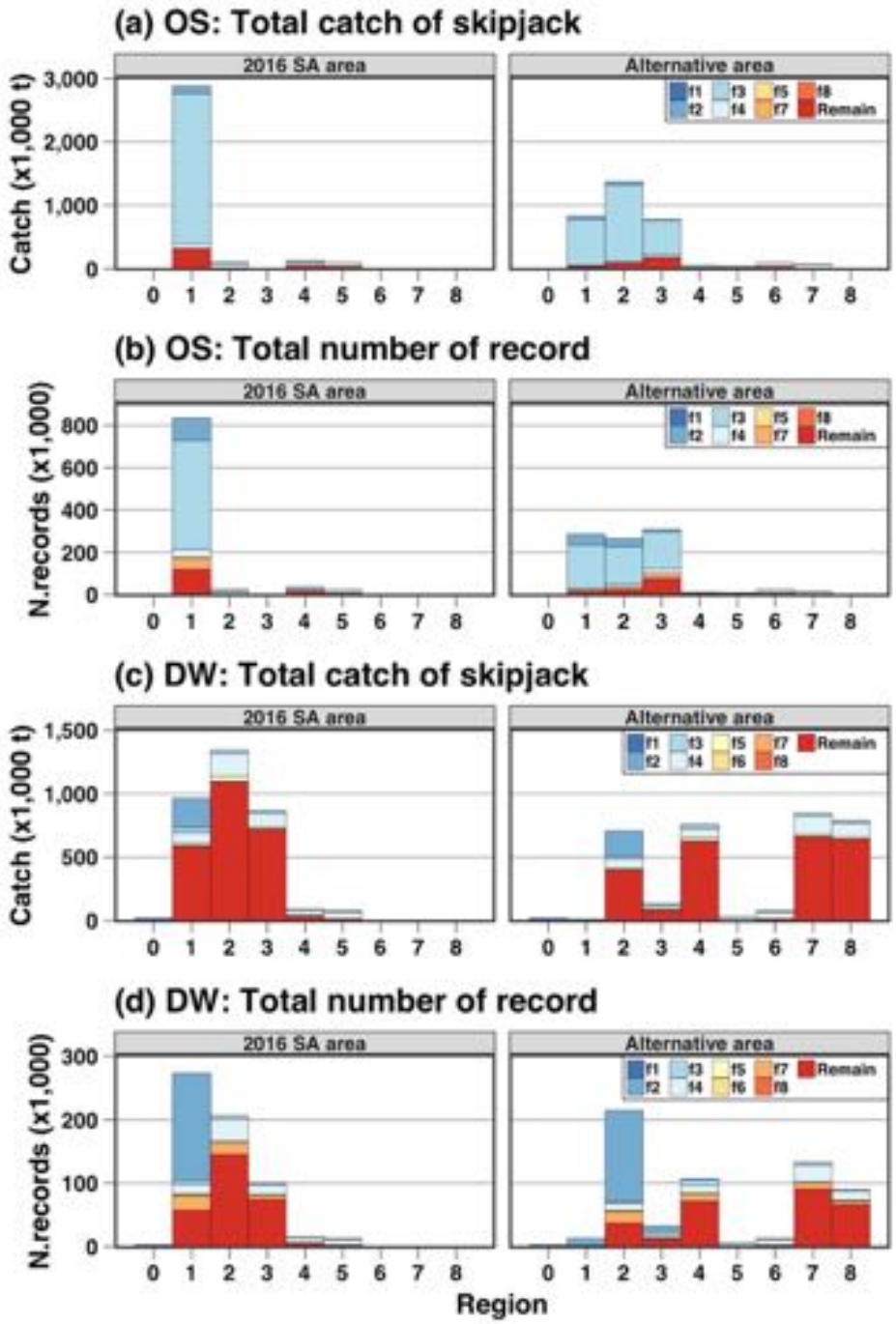

Figure 5. Ratio of filtered data at each filtering step in each region (a) total catch made by OS, (b) number of records reported by OS, (c) total catch made by DW, and (d) number of records reported by DW. Region 0 was used to indicate data outside of the WCPO. Remain as shown in red presents the data remained after all the filtering processes were applied, which were used as the input data for the model with the screening procedure 1 (SP1). The abbreviations of f1–f8 in the figure indicate that catch (a, c) and number of records (b, d) filtered out by applying Filter 1–Filter 8, respectively (for details of filters, refer to the text).

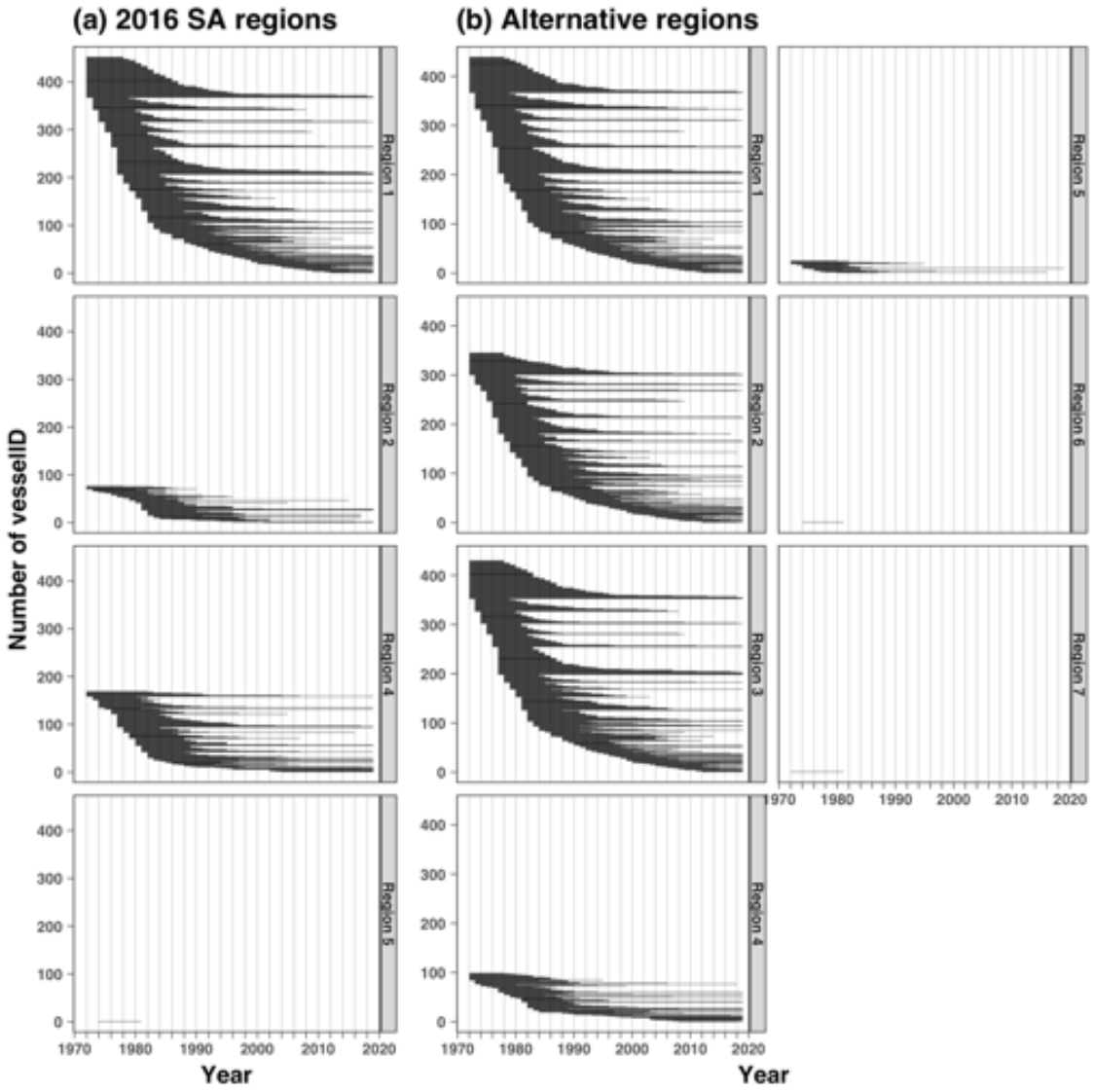

Figure 6. Active duration of every JPNPL OS vessel ID in each regional definition used in (a) the 2016 SA and (b) the alternative with SP2 model input.

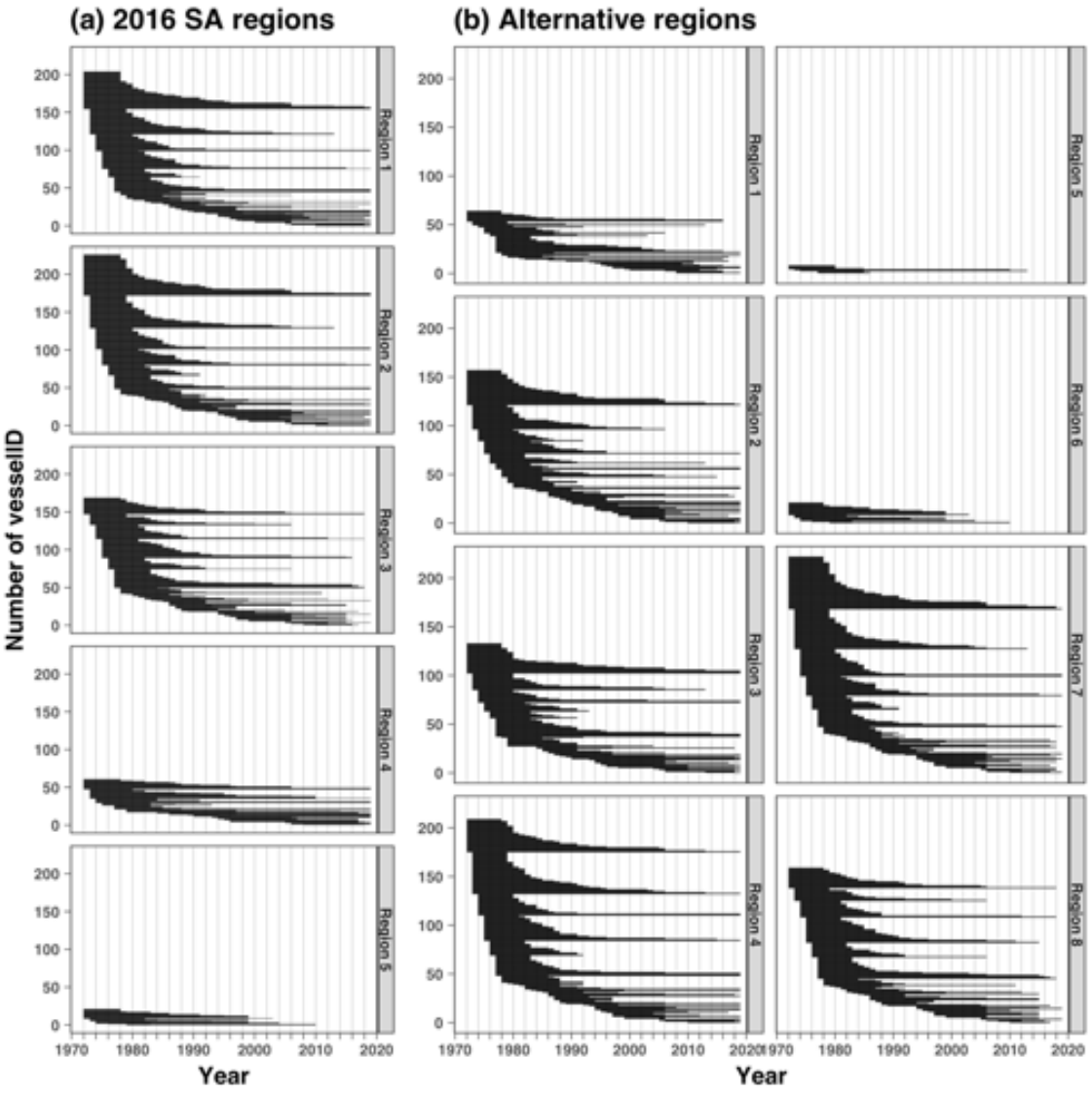

Figure 7. Active duration of every JPNPL DW vessel ID in each regional definition used in (a) the 2016 SA and (b) the alternative with SP2 model input.

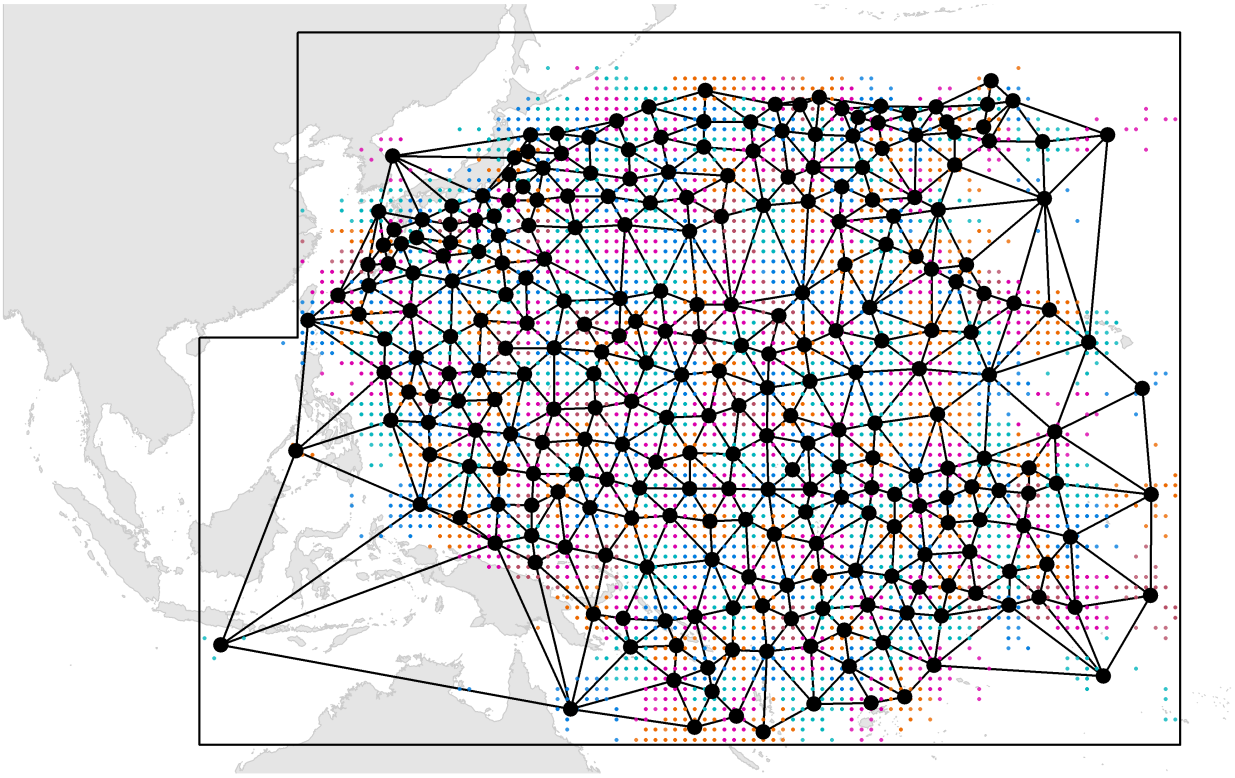

Figure 8. Triangular mesh and spatial knot structure used for the geostats model. Knots (black dots) were allocated in proportion to the density of fishing effort with knots being placed closer together in areas of highest concentration of fishing effort. The colored dots indicate 1×1° grid cells with spatial observations from either the DW or OS components of the fleet.

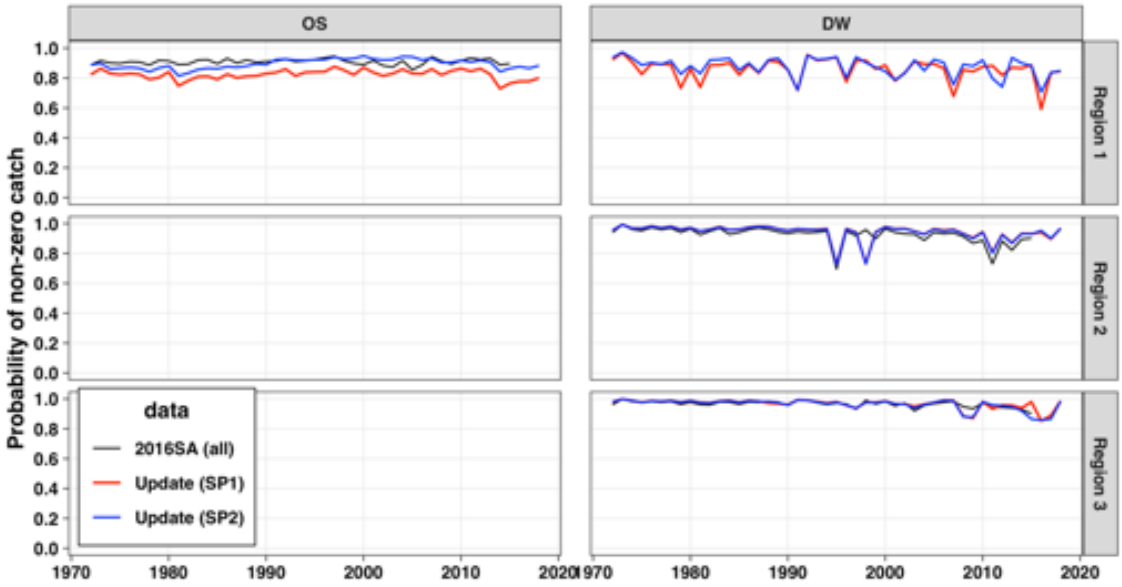

Figure 9. Probability of non-zero catch (the binomial part of the model) in the 2016 SA spatial structure using the delta-GLM model.

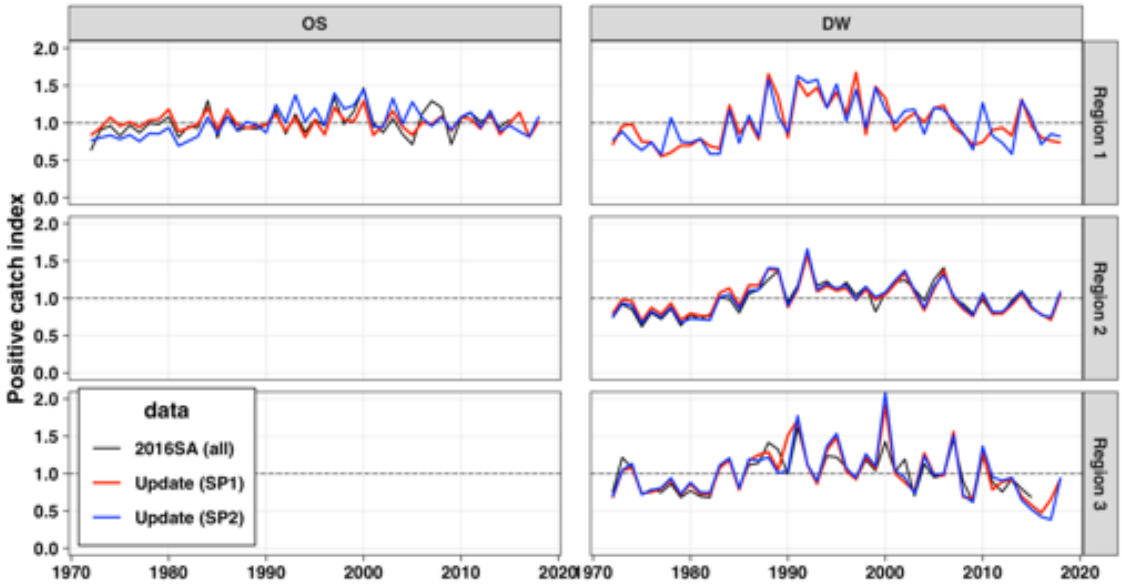

Figure 10. Positive index (the lognormal part of the model) obtained in the 2016 SA spatial structure using the delta-GLM model.

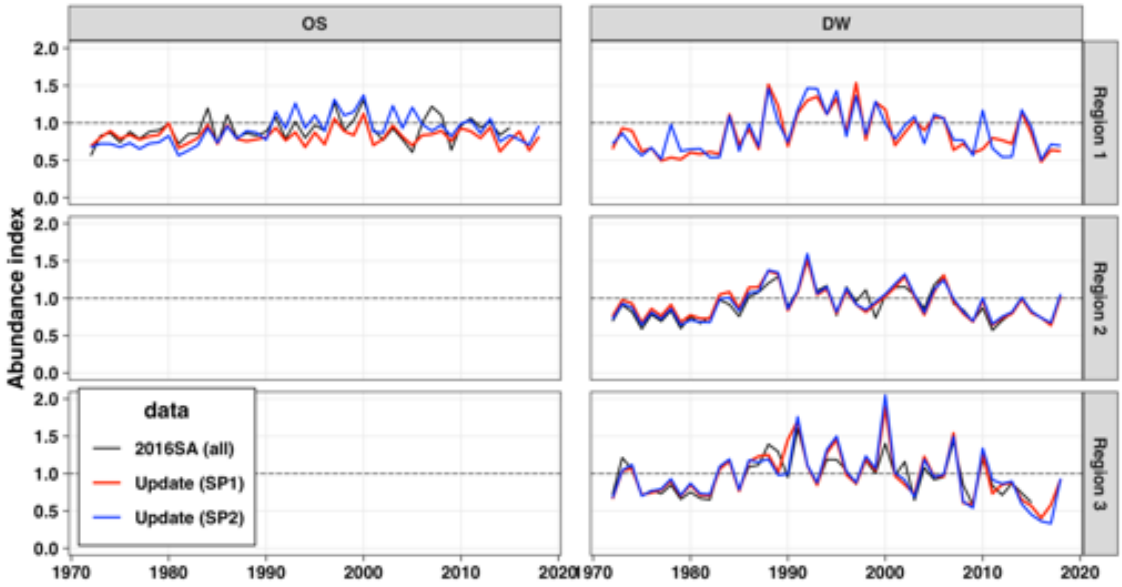

Figure 11. Abundance index (i.e., the standardized CPUE) of JPNPL obtained in the 2016 SA spatial structure using the delta-GLM model.

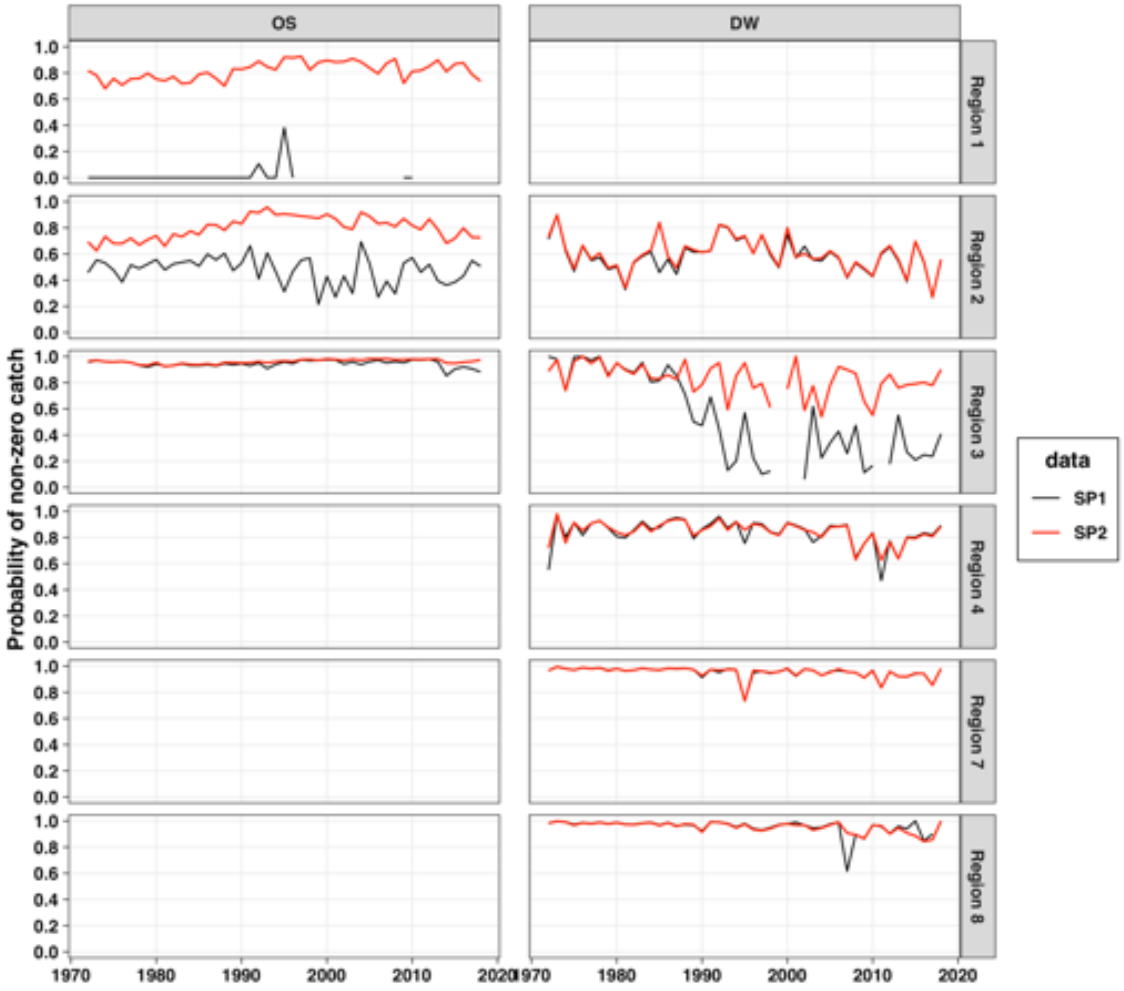

Figure 12. Probability of non-zero catch (the binomial part of the model) obtained in the alternative spatial structure using the delta-GLM model.

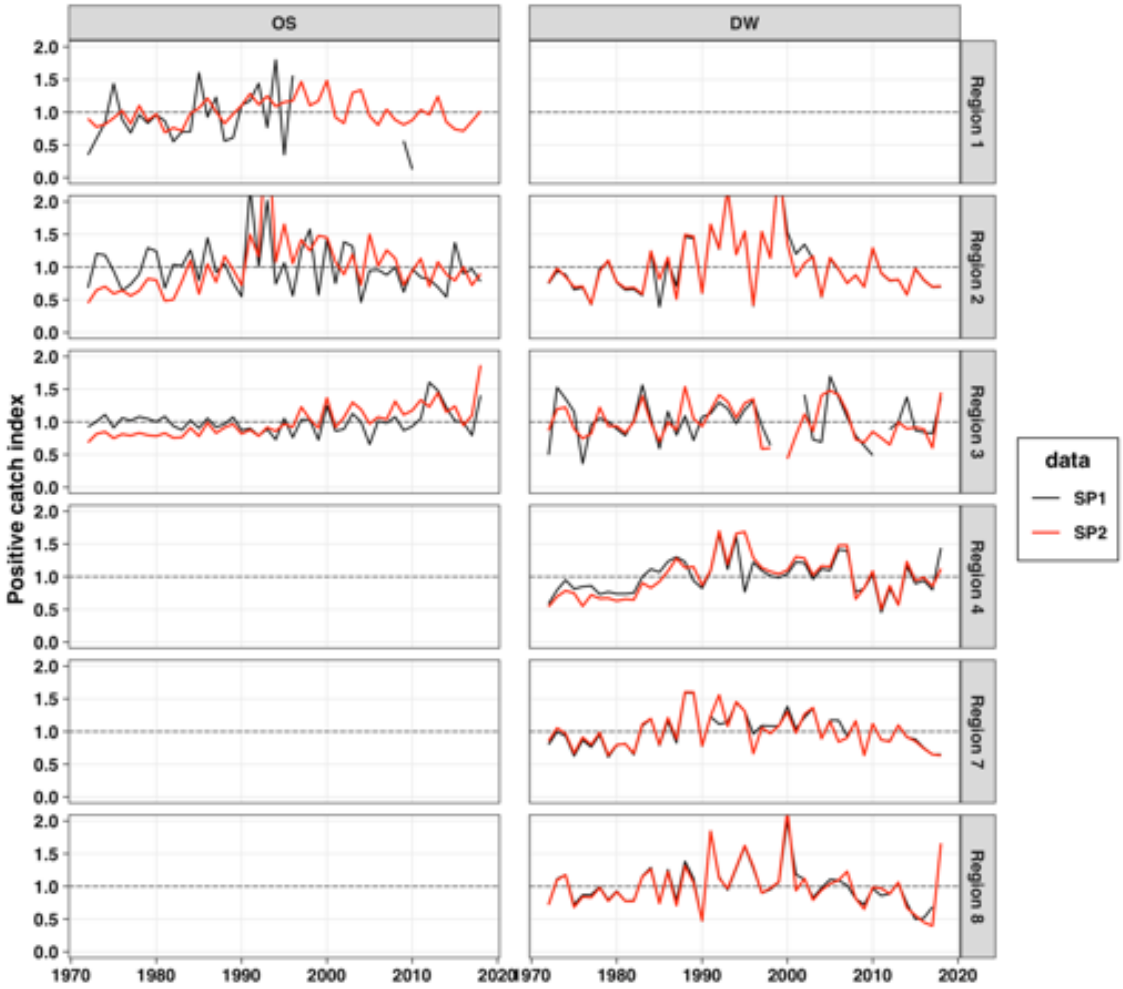

Figure 13. Positive index (the lognormal part of the model) obtained in the alternative spatial structure using the delta-GLM model.

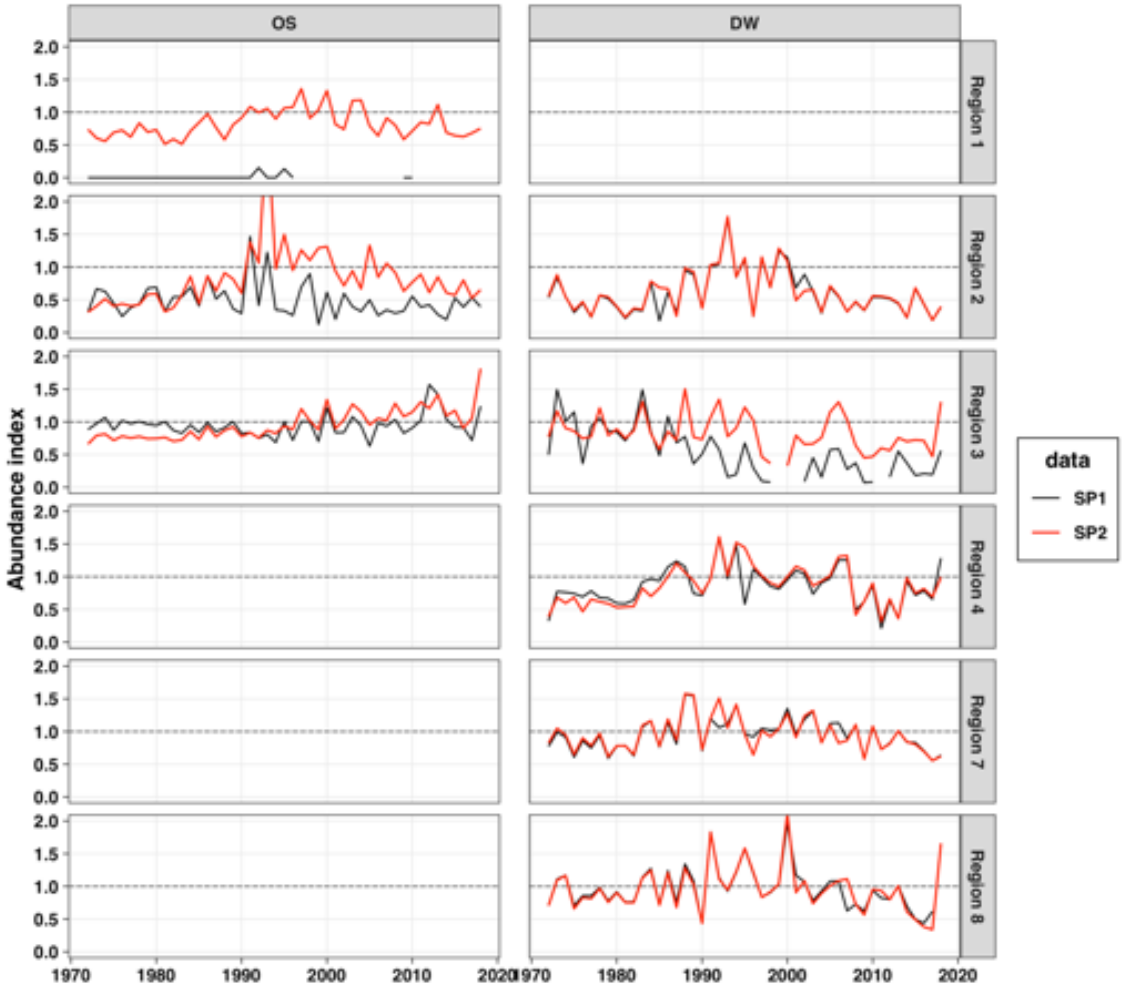

Figure 14. Abundance index (i.e., the standardized CPUE) of JPNPL obtained in the alternative spatial structure using the delta-GLM model.

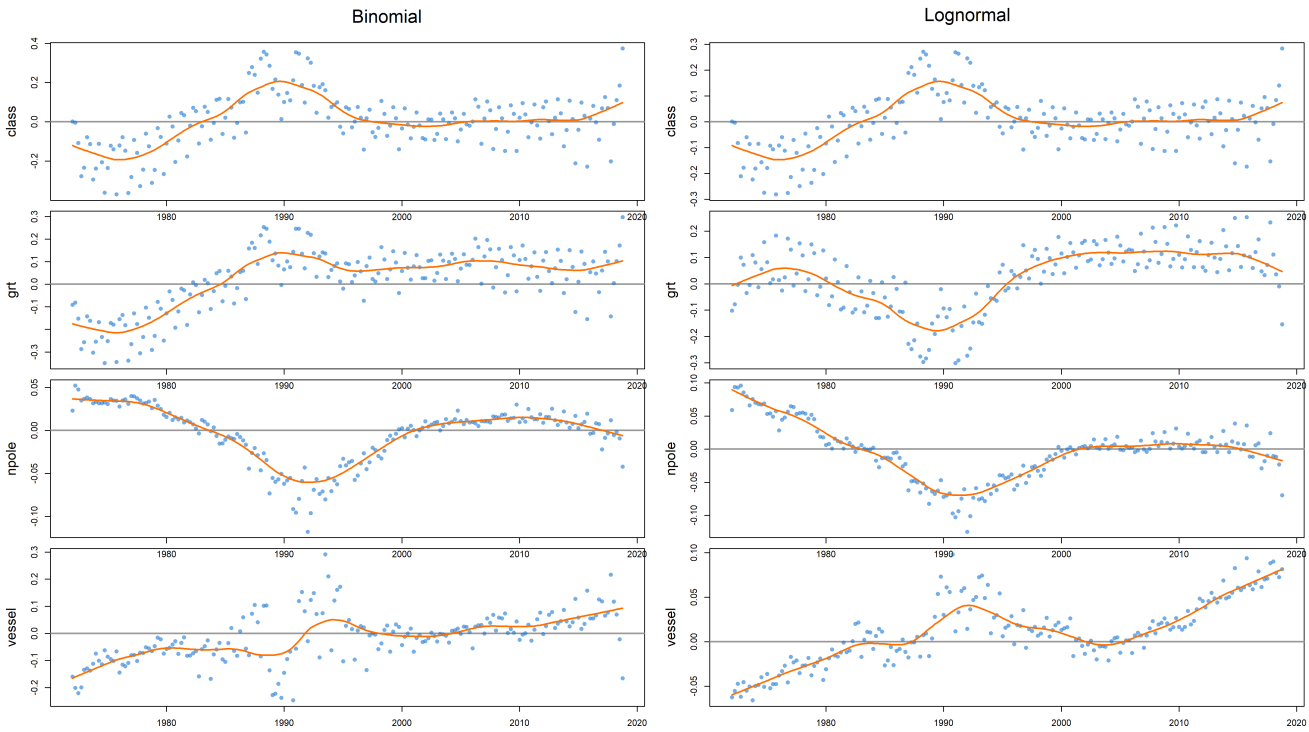

Figure 15. Influence plot showing the relative effect of each covariate over time for both the binomial and lognormal component of the geostats model. The colored dots represent the covariate effect for each year-quarter and the colored line is the loess trend through the data. The horizontal line indicates the mean effect for that covariate. Additionally the units are the same in each plot allowing for comparison of the magnitude of the effect between covariates.

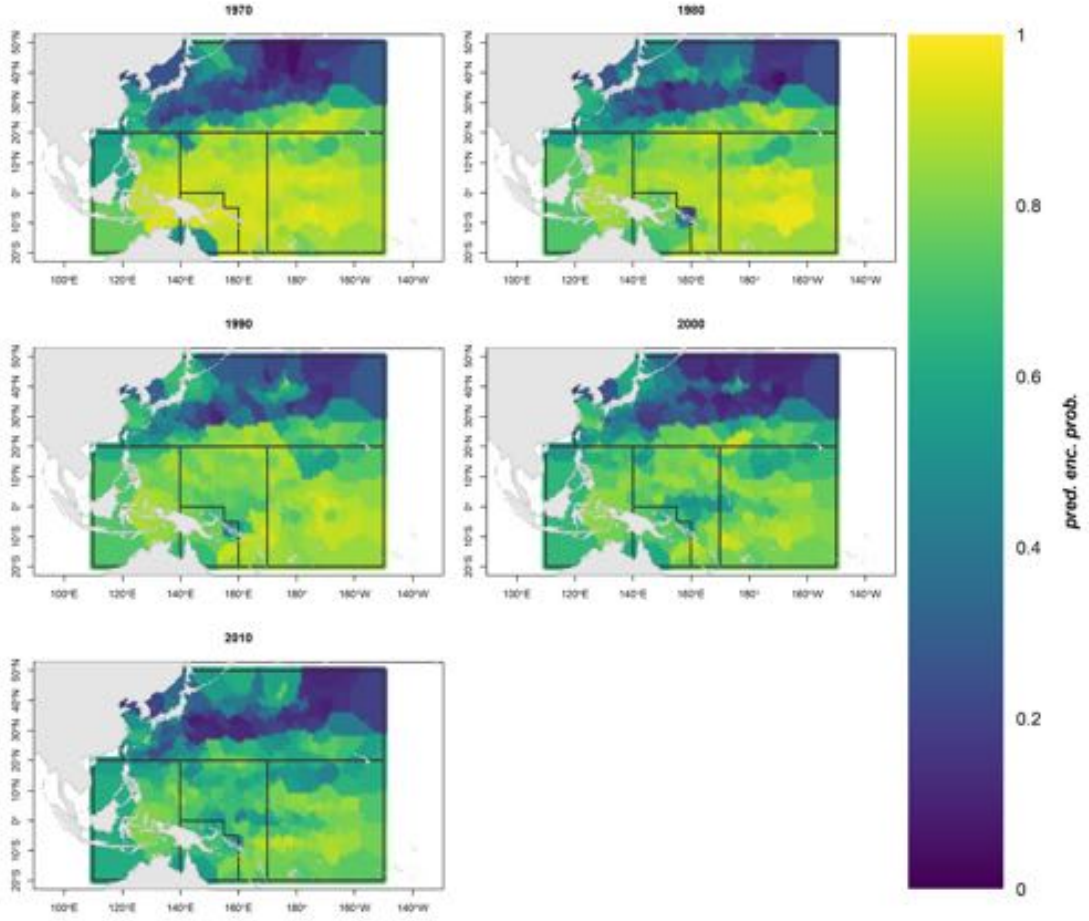

Figure 16. Predicted spatial probability of encounter (binomial component) of skipjack by decade from the geostats model for each 1×1° grid cell. Warmer colors indicate a greater probability of encounter, and cooler colors indicate a lower probability of encounter.

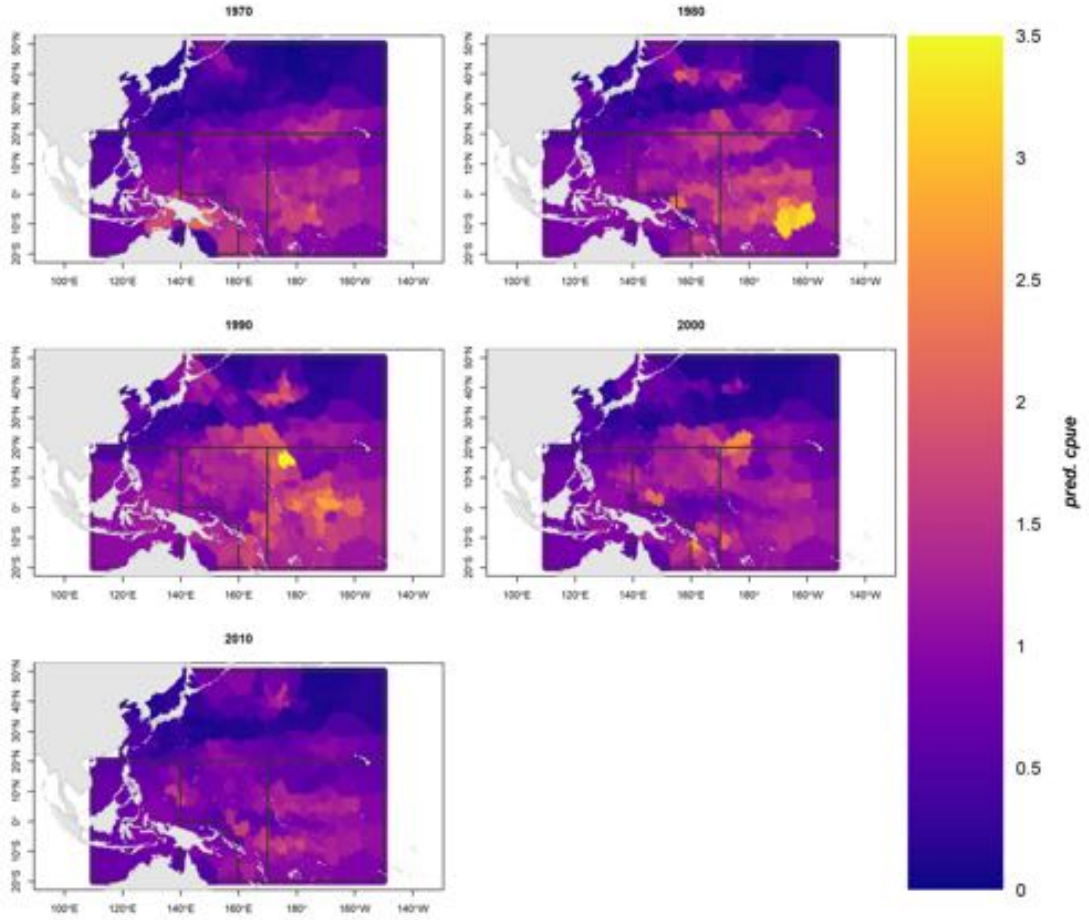

Figure 17. Predicted spatial CPUE of skipjack by decade from the geostats model for each 1×1° grid cell. Warmer colors indicate higher CPUE (metric tons per day), and cooler colors indicate lower CPUE.

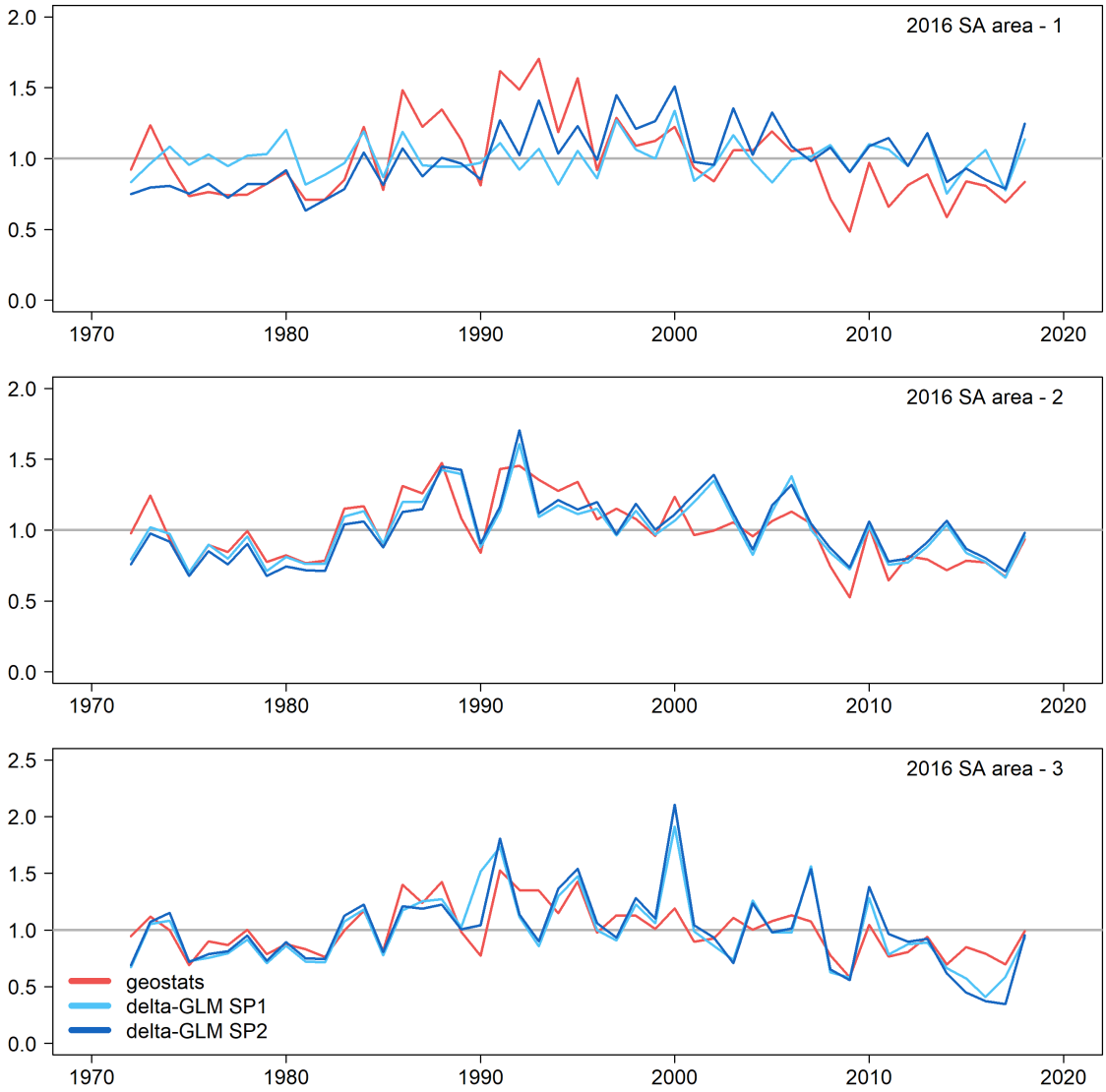

Figure 18. Mean centered, standardized indices of abundance for each of the three main model formulations for the 2016 SA spatial structure: geostats (red), delta-GLM SP1 (light blue), and delta-GLM SP2 (dark blue).

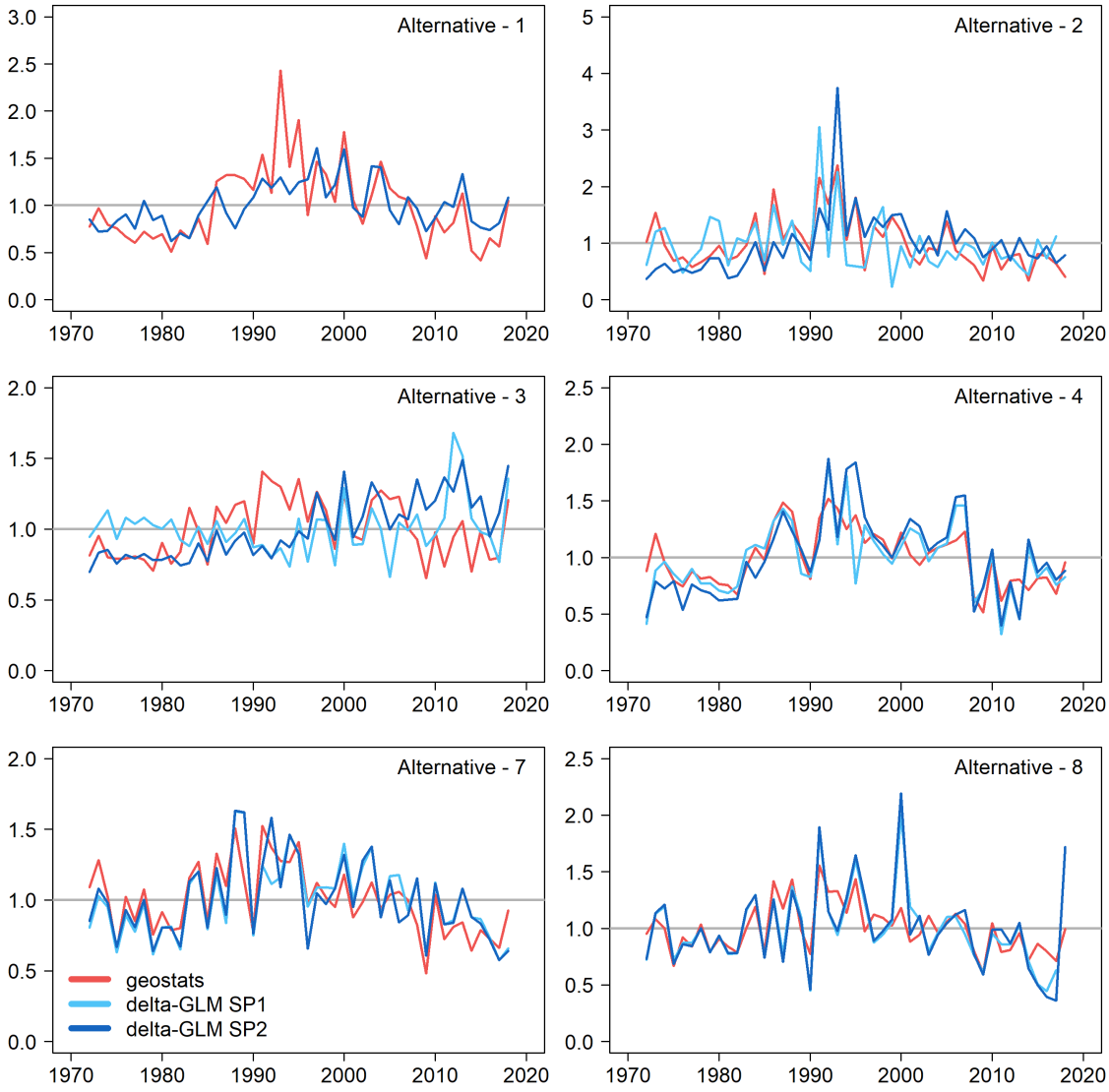

Figure 19. Mean centered, standardized indices of abundance for each of the three main model formulations for the 2019 alternative spatial structure: geostats (red), delta-GLM SP1 (light blue), and delta-GLM SP2 (dark blue).